Computational Visual Media
https://doi.org/10.1007/s41095-020-0182-8 Vol. 6, No. 3, September 2020, 349–354

Short Communication

Designing planar cubic B-spline curves with monotonic curvature for curve interpolation

Aizeng Wang[1,2], Chuan He[1,2], Fei Hou[3,4], Zhanchuan Cai[5], and Gang Zhao[1,2] (✉)

Monotonic curvature plays an important role in industrial design and styling of curves with aesthetic shapes, e.g., in automobile and aircraft design [1]. Used in conventional parametric CAD/CAM systems, general B-splines are not adequate for aesthetic requirements. Except for the straight line and circle, monotonic curvature distribution, associated with pleasing shape, is very difficult to achieve.

So Farin suggested that a fair curve has a curvature plot with relatively few regions of monotonically varying curvature. Starting from this basis, work on B-spline fairing was developed mainly in three direction: knot-removal-reinsertion methods, optimization methods based on minimizing an energy function, and filtering approaches based on B-spline wavelets.

Visual curve completion (interpolating a curve segment, with continuity, to fill a gap) is a fundamental problem for human visual understanding [2]. Aesthetically pleasingly shaped curves usually have monotonically varying curvature [3]. While the shape of a curve is primarily defined by its curvature distribution, monotonicity of curvature is not easily achieved and controlled. To overcome this problem, we present a construction approach for B-spline curves, which guarantees monotonic curvature by enforcing simple geometric constraints on the control vectors.

Euler curves have the useful property that their curvature changes linearly with arc length, so are widely used in modeling and shape interpolation [4–6]. However, Euler curves also have disadvantages for curve interpolation. Firstly, they are defined by transcendental functions, requiring complex mathematical expressions which are difficult to compute. Secondly, given two endpoints with associated tangents, there is no exact solution for an Euler curve. Thirdly, Euler curves are not compatible with current CAD software systems, which are based on NURBS. In order to overcome these drawbacks of Euler curves, we have developed a new interpolation algorithm for cubic B-spline curves, with advantages of simple computation, exact interpolation and compatibility with existing CAD systems.

1 School of Mechanical Engineering & Automation, Beihang University, Beijing 100191, China. E-mail: A. Wang, azwang@buaa.edu.cn; C. He, hc1994@buaa.edu.cn; G. Zhao, zhaog@buaa.edu.cn (✉).

2 State Key Laboratory of Virtual Reality Technology & Systems, Beihang University, Beijing 100191, China.

3 State Key Laboratory of Computer Science, Institute of Software, Chinese Academy of Sciences, Beijing 100190, China. E-mail: houfei@ios.ac.cn.

4 University of Chinese Academy of Sciences, Beijing 100049, China.

5 Faculty of Information Technology, Macau University of Science and Technology, Macau 999078, China. E-mail: zccai@must.edu.mo.

Manuscript received: 2020-02-25; accepted: 2020-05-19

1 Planar cubic B-spline curves with monotonic curvature

1.1 Theory

In this paper, we consider cubic curves. A planar B-spline curve of degree three is defined by

$$P(t) = \sum_{i=0}^{n} C_i N_{i,3}(t) = \sum_{i=j-3}^{j} C_i N_{i,3}(t), \quad t \in [t_j, t_{j+1}] \subset [t_3, t_{n+1}] \tag{1}$$

where C_i are control points (see Fig. 1(a)), and $N_{i,3}(t)$ are B-spline basis functions defined on the knot vector $t = [t_0, \ldots, t_{n+3}]$. The derivatives of this curve can

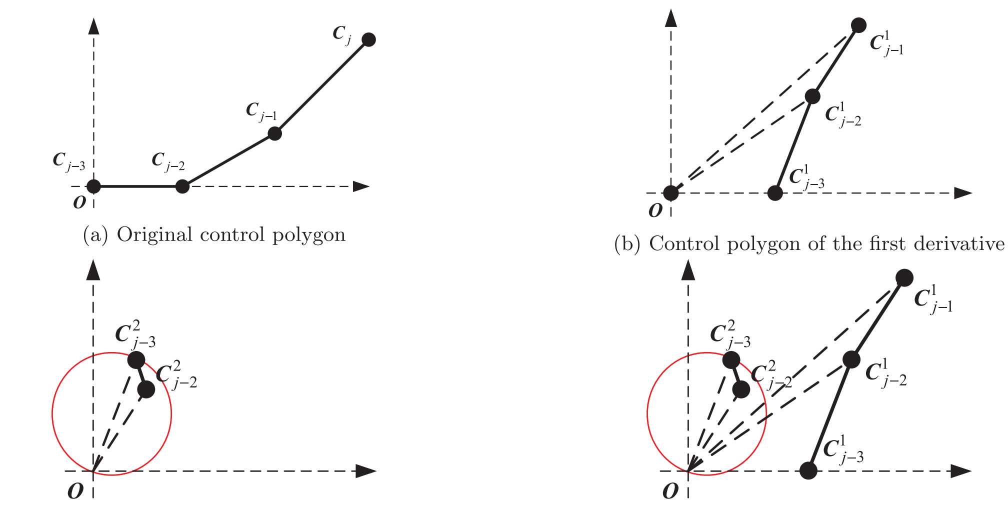

(a) Original control polygon

(b) Control polygon of the first derivative

(c) Control polygon of the second derivative

(d) $\angle\langle P'(t), P''(t)\rangle$

Fig. 1 Control polygons of a cubic B-spline curve and its derivatives.

be expressed as

$$\begin{aligned} P'(t) &= \sum_{i=0}^{n-1} C_i^1 N_{i,2}(t) \\ &= \sum_{i=j-2}^{j} C_i^1 N_{i,2}(t), \quad t \in [t_j, t_{j+1}] \subset [t_3, t_{n+1}] \end{aligned} \tag{2}$$

$$\begin{aligned} C_i^1 &= \frac{3-1+1}{u_{i+3+1} - u_{i+1}}(C_{i+1} - C_i) \\ &= \frac{3}{u_{i+4} - u_{i+1}}(C_{i+1} - C_i) \end{aligned} \tag{3}$$

where $P'(t)$ is the first derivative of the B-spline curve, and C_i^1 represents its corresponding control points (see Fig. 1(b)). Proceeding further, we obtain

$$\begin{aligned} P''(t) &= \sum_{i=0}^{n-2} C_i^2 N_{i,1}(t) \\ &= \sum_{i=j-1}^{j} C_i^2 N_{i,1}(t), \quad t \in [t_j, t_{j+1}] \subset [t_3, t_{n+1}] \end{aligned} \tag{4}$$

$$\begin{aligned} C_i^2 &= \frac{3-2+1}{u_{i+3+1} - u_{i+2}}(C_{i+1}^1 - C_i^1) \\ &= \frac{2}{u_{i+4} - u_{i+2}}(C_{i+1}^1 - C_i^1) \end{aligned} \tag{5}$$

where $P''(t)$ is the second derivative, and C_i^2 represents the corresponding control points (see Fig. 1(c)).

Now consider a B-spline curve segment with four control points. It can be represented as $P(t) = \sum_{i=j-3}^{j} C_i N_{i,3}(t)$, $t \in [t_j, t_{j+1}]$. We construct a local coordinate system. Specifically, let the direction of the first control vector be the x-axis, and C_{j-3} be the origin (see Fig. 2).

Next, we prove that if the following three geometrical Lemmas are satisfied, the B-spline curve segment on $[t_j, t_{j+1}]$ has monotonic curvature.

Lemma 1. If the first and second derivative control points $\{C_{j-3}^1, C_{j-2}^1, C_{j-1}^1\}$ and $\{C_{j-3}^2, C_{j-2}^2\}$ are located in the same quadrant (see Figs. 1(b) and 1(c)), then $\| P'(t) \|' \geqslant 0$ for $t \in [t_j, t_{j+1}]$.

Proof. From $\| P'(t) \| = (P'(t)(P'(t))^{\mathrm{T}})^{1/2}$, we can derive

$$\| P'(t) \|' = \frac{P'(t)(P''(t))^{\mathrm{T}}}{\| P'(t) \|} \tag{6}$$

Thus, if $P'(t)$ and $P''(t)$ are in the same quadrant, then $\| P'(t) \|' \geqslant 0$ for $t \in [t_j, t_{j+1}]$. □

Lemma 2. If angle $\angle OC_{j-2}^2 C_{j-3}^2 \geqslant \pi/2$ (see Fig. 1(c)), then $\| P''(t) \|' \leqslant 0$ for $t \in [t_j, t_{j+1}]$.

Proof. Because $\angle OC_{j-2}^2 C_{j-3}^2 \geqslant \pi/2$, it can be inferred that $\| OC_{j-3}^2 \| \geqslant \| OC_{j-2}^2 \|$. As

$$\| P''(t) \| = \frac{t_{j+1} - t}{t_{j+1} - t_j} \| OC_{j-3}^2 \| + \frac{t - t_j}{t_{j+1} - t_j} \| OC_{j-2}^2 \|$$

we have $\| P''(t + \Delta t) \| \leqslant \| P''(t) \|$, where $\Delta t \geqslant 0$ and $t \in [t_j, t_{j+1}]$. Thus, $\| P''(t) \|' \leqslant 0$ for $t \in [t_j, t_{j+1}]$. □

Lemma 3. If $s_{\overline{OC_{j-2}^1}} \leqslant s_{\overline{C_{j-2}^1 C_{j-1}^1}} \leqslant s_{\overline{C_{j-3}^1 C_{j-2}^1}}$, where s denotes slope (see Fig. 1(d)), then

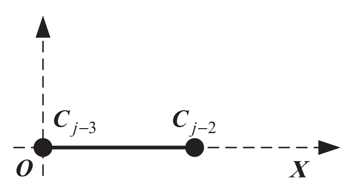

Fig. 2 Local coordinate system for a curve segment.

$\sin(\langle P'(t), P''(t)\rangle) \leqslant 0$ for $t \in [t_j, t_{j+1}]$, where $\langle\rangle$ denotes the angle between two vectors.

Proof. As the vector $C^1_{j-2}C^1_{j-1} = OC^2_{j-2}$ and $C^1_{j-3}C^1_{j-2} = OC^2_{j-3}$, we have $s_{\overline{OC^1_{j-2}}} \leqslant s_{\overline{OC^2_{j-2}}} \leqslant s_{\overline{OC^2_{j-3}}}$. If $s_{\overline{OC^1_{j-2}}} \leqslant s_{\overline{C^1_{j-2}C^1_{j-1}}} \leqslant s_{\overline{C^1_{j-3}C^1_{j-2}}}$, from the variation diminishing property, we can derive that $0 \leqslant \angle\langle P'(t+\Delta t), P''(t+\Delta t)\rangle \leqslant \angle\langle P'(t), P''(t)\rangle \leqslant \pi/2$, where $\Delta t \geqslant 0$, $t \in [t_j, t_{j+1}]$. Then, $\sin\langle P'(t+\Delta t), P''(t+\Delta t)\rangle \leqslant \sin(\langle P'(t), P''(t)\rangle)$. Thus, $\sin(\langle P'(t), P''(t)\rangle)$ is decreasing for $t \in [t_j, t_{j+1}]$. □

We may now prove the following theorems.

Theorem 1. If a B-spline control polygon satisfies Lemmas 1–3, then the curvature of the curve segment is monotonic.

Proof. If Lemmas 1–3 are satisfied, then (i) $\| P'(t) \|' \geqslant 0$, (ii) $\| P''(t) \|' \leqslant 0$, and (iii) $\sin(\langle P'(t), P''(t)\rangle)' \leqslant 0$ for $t \in [t_j, t_{j+1}]$. Then, we can conclude that $\kappa(t+\Delta t) \leqslant \kappa(t)$ as

$$\kappa(t) = \frac{\| P''(t) \| \sin\langle P'(t)P''(t)\rangle}{\| P'(T) \|^2}$$

where $\Delta t \geqslant 0$. Therefore, the curvature $\kappa(t)$ is a decreasing function for $t \in [t_j, t_{j+1}]$, and this curve segment has monotonic curvature. □

Theorem 2. If (i) C^2_{j-2} is located in a fair location (defined in Fig. 3), (ii) $s_{\overline{OC^1_{j-2}}} \leqslant s_{\overline{OC^2_{j-3}}}$, and (iii) $\{C^1_{j-3}, C^1_{j-2}, C^1_{j-1}\}$ and $\{C^2_{j-3}, C^2_{j-2}\}$ are located in the same quadrant, then the curvature of the associated B-spline curve segment on $[t_j, t_{j+1}]$ is monotone.

Proof. If the given geometric conditions are satisfied, we have (i) $\{C^1_{j-3}, C^1_{j-2}, C^1_{j-1}\}$ and $\{C^2_{j-3}, C^2_{j-2}\}$ are located in the same quadrant, (2) angle $\angle OC^2_{j-2}C^2_{j-3} \geqslant \pi/2$, because C^2_{j-2} is located within the red circle with diameter OC^2_{j-3}, and (iii) $s_{\overline{OC^1_{j-2}}} \leqslant s_{\overline{OC^2_{j-2}}} = s_{\overline{C^1_{j-2}C^1_{j-1}}} \leqslant s_{\overline{OC^2_{j-3}}} = s_{\overline{C^1_{j-3}C^1_{j-2}}}$ (see Fig. 3). Thus, Theorem 1 is satisfied by the B-spline curve segment, proving the result. □

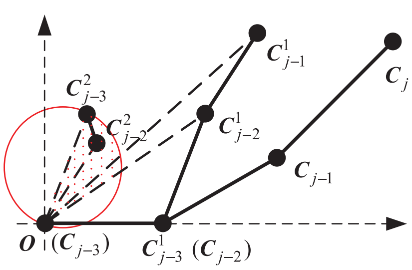

Fig. 3 Fair location. C^2_{j-2} is in a fair location if it lies within the red dashed region, which is bounded by OC^2_{j-3}, OC^1_{j-2}, and the red circle with diameter OC^2_{j-3}.

From Theorem 2, if $\| C^1_{j-2}C^1_{j-1} \| \leqslant \| C^1_{j-3}C^1_{j-2} \|$ and $C^1_{j-2}C^1_{j-1} \parallel C^1_{j-3}C^1_{j-2}$ are enforced (see Fig. 4), the control polygon satisfies the three geometric conditions. Thus, the corresponding B-spline curve segment has monotonic curvature.

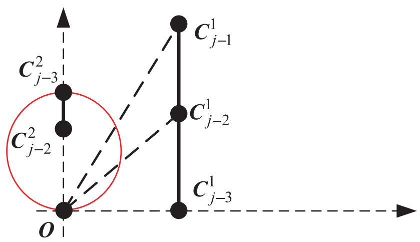

Fig. 4 A special case of Theorem 2.

1.2 Designing cubic B-spline curves with monotonic curvature

Using the result in Theorem 2 as a basis, our design approach may be summarized in the following steps.

1. Fix the first B-spline control vector. Let $\boldsymbol{V}_0 = C_1 - C_0$ (see Fig. 5);
2. Fix the second vector. Let $\boldsymbol{V}_1 = C_2 - C_1$, where $\boldsymbol{V}_0$ and $\Delta\boldsymbol{V}_0 = \boldsymbol{V}_1 - \boldsymbol{V}_0$ are located in the same quadrant (see Fig. 6);
3. Fix the third vector. Let $\boldsymbol{V}_2 = C_3 - C_2$, where $s_{\overline{OC^1_1}} \leqslant s_{\overline{OC^2_0}}$, and $\Delta\boldsymbol{V}_1 = \boldsymbol{V}_2 - \boldsymbol{V}_1(C^2_1)$ is located in a fair location (see Fig. 7);
4. Fix the i-th vector. For a B-spline, if $\boldsymbol{V}_{i-2}$ and $\boldsymbol{V}_{i-1}$ are given, $\boldsymbol{V}_i$ can be determined by steps (1)–(3).

Our design algorithm for a B-spline curve segment satisfies Lemmas 1–3 and hence Theorem 1: (i)

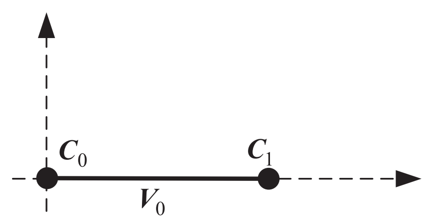

Fig. 5 Determine the initial B-spline control vector.

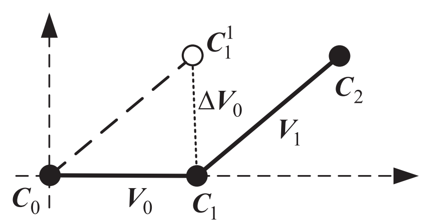

Fig. 6 Determine the second control vector.

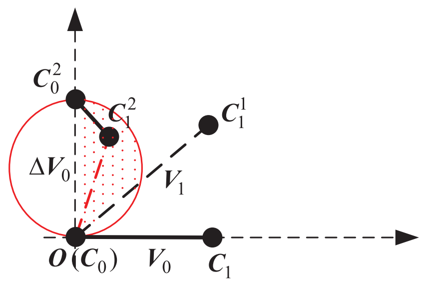

Fig. 7 Determine the third control vector.

$\{C^1_{j-3}, C^1_{j-2}, C^1_{j-1}\}$ and $\{C^2_{j-3}, C^2_{j-2}\}$ are located in the same quadrant, (ii) $s_{\overline{OC^1_{j-2}}} \leqslant s_{\overline{OC^2_{j-2}}} \leqslant s_{\overline{OC^2_{j-3}}}$, and (iii) $\angle OC^2_{j-2}C^2_{j-3} \geqslant \pi/2 (j = 3, \ldots, n)$. Therefore, the designed curve has monotonic curvature.

Pseudocode is given in Algorithm 1.

Algorithm 1

Input: number of control edges n, knot vector t, and initial conditions.
Output: planar cubic B-spline curve with monotonic curvature.
Initialize: $C_0 = (0, 0, 0)$, $C_1 = (a, 0, 0)$, and $\boldsymbol{V}_0 = C_1 - C_0$, where $a > 0$
input $\Delta\boldsymbol{V}_0 = \boldsymbol{V}_1 - \boldsymbol{V}_0$ lying in the first quadrant
for $i = 1$ **to** $n - 1$ **do**
  input $\Delta\boldsymbol{V}_i = \boldsymbol{V}_{i+1} - \boldsymbol{V}_i$ in a fair location
end for

1.3 Curve interpolation with B-spline curves with monotonic curvature

We now consider curve interpolation: given two specified endpoints with associated tangent directions, we wish to find a curve satisfying these G^1 conditions. See Algorithm 2, which uses a knot sequence which is uniformly spaced everywhere except at its ends. Due to affine invariance, without loss of generality we can fix the origin at the initial control point C_0, and set the x axis to the tangent direction T_0 (see Fig. 8). The end control point should be located in the first quadrant with a proper tangent direction, limited between the two dashed lines (see Fig. 8).

We proceed as follows. Compute the intersection M of the two tangent directions. Select parameters t_1, t_{2x}, t_{2y}, and t_3 for the middle three control points respectively. Set $C_1 = t_1P$, $C_3 = (1 - t_3)M + t_3C_4$, $C_2 = (t_{2x}C_4.x, t_{2y}C_4.y)$ (see Fig. 9). From Eqs. (3), (5), and Lemma 1, we can deduce that $0 < t_1 < 1/6$, $0 < t_3 < 4/5$, $3t_1 < t_{2x} < C_3.x/C_4.x$, $0 < t_{2y} < 1/2t_3$. As long as the intersection point M is located between the two dashed lines in Fig. 8, this can always be done.

Algorithm 2

Input: two endpoints with associated tangent directions (see Fig. 8)
Output: planar cubic B-spline segment with monotonic curvature.
Initialize: $\delta = 0.02, n = 4$

for $t_1 = 0$ to $1/6$ step δ **do**
  $C_1 = t_1P$
  for $t_3 = 0$ to $4/5$ step δ **do**
    $C_3 = (1 - t_3)M + t_3C_4$
    for $t_{2x} = 3t_1$ to $C_3.x/C_4.x$ step δ **do**
      $C_2.x = t_{2x}C_4.x$
      for $t_{2y} = 0$ to $t_3/2$ step δ **do**
        Success = False
        $C_2.y = t_{2y}C_4.y$
        $C_2 = (C_2.x, C_2.y)$
        Compute C_i^1, C_i^2
        if (C_i^1 and C_i^2 satisfy Lemmas 1–3) **then**
          return control points
        end if
      end for
    end for
  end for
end for

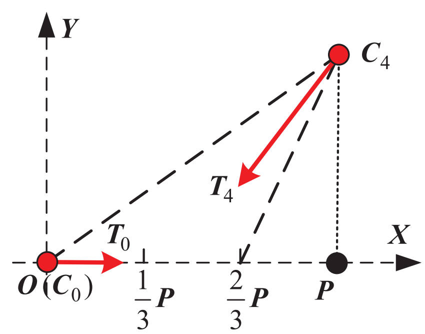

Fig. 8 Given data to interpolate.

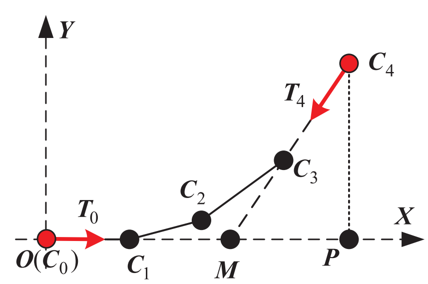

Fig. 9 Generating the middle control points.

2 Examples of curve interpolation

This section gives examples to demonstrate the effectiveness of our new design approach.

The first example is a cubic B-spline curve with five control points (see Fig. 10(a)). From Theorem 1, it can be inferred that the B-spline curve has monotonic curvature, as confirmed in Fig. 10(b).

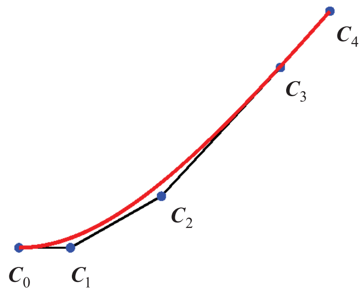

(a) Generated B-spline curve

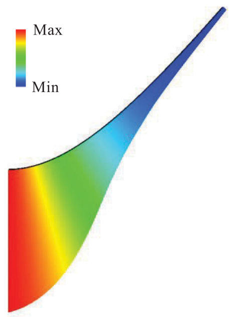

(b) Its curvature comb

Fig. 10 Designing a B-spline curve using Algorithm 1.

Figures 11–13 show applications of Algorithm 2 to curve completion for occluded objects. Figure 11(a) is a partially occluded bird; in Fig. 11(b) we use a cubic B-spline curve constructed by our method to complete its boundary. Figure 12 shows an example of leaf vein completion. Lastly, the curve in Fig. 13 completes the edge of a wine glass in an artistic photograph.

(a) Partially occluded bird

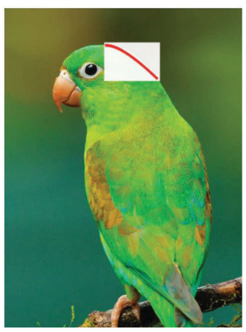

(b) Boundary curve completion

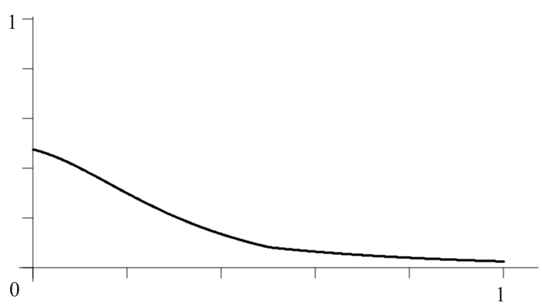

(c) Corresponding curvature plot

Fig. 11 Bird silhouette completion using Algorithm 2.

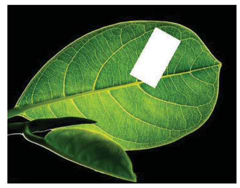

(a) Partially occluded leaf

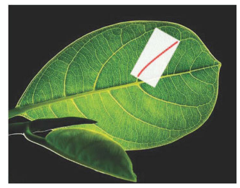

(b) Leaf vein completion

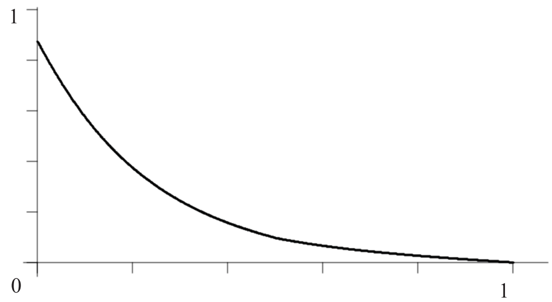

(c) Corresponding curvature plot

Fig. 12 Leaf vein completion using Algorithm 2.

(a) Partially occluded wine glass

(b) Silhouette completion

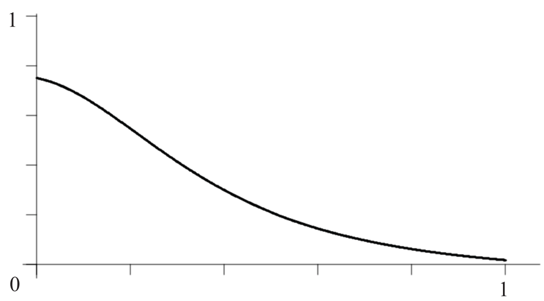

(c) Corresponding curvature plot

Fig. 13 Wine glass silhouette completion using Algorithm 2.

Acknowledgements

This work was supported by the Opening Fund of the State Key Laboratory of Lunar and Planetary

Sciences, Macau University of Science and Technology (Macau FDCT Grant No. 119/2017/A3), the Open Project Program of the State Key Lab of CAD&CG, Zhejiang University (No. A2024), the National Natural Science Foundation of China (Nos. 61572056, 61872347), and the Special Plan for the Development of Distinguished Young Scientists of ISCAS (No. Y8RC535018).

References

[1] Birkhoff, G. D. *Aesthetic Measure*. Harvard University Press, 1933.

[2] Lin, H. W.; Wang, Z. H.; Feng, P. P.; Lu, X. J.; Yu, J. H. A computational model of topological and geometric recovery for visual curve completion. *Computational Visual Media* Vol. 2, No. 4, 329–342, 2016.

[3] Farin, G. *Curves and Surfaces for Computer-Aided Geometric Design: A Practical Guide*. Elsevier, 2014.

[4] Harary, G.; Tal, A. The natural 3D spiral. *Computer Graphics Forum* Vol. 30, No. 2, 237–246, 2011.

[5] Zhou, H. L.; Zheng, J. M.; Yang, X. N. Euler arc splines for curve completion. *Computers & Graphics* Vol. 36, No. 6, 642–650, 2012.

[6] Harary, G.; Tal, A. 3D Euler spirals for 3D curve completion. *Computational Geometry* Vol. 45, No. 3, 115–126, 2012.

Aizeng Wang is currently an associate professor in the School of Mechanical Engineering & Automation, Beihang University. He received his Ph.D. degree from Beihang University, and was a postdoc at Nanyang Technological University of Singapore. His research interests include geometry processing, class A curves & surfaces, and wavelet analysis.

Chuan He is a graduate student in the School of Mechanical Engineering & Automation, Beihang University. His research interests include class A curves and surfaces, T-splines, and wavelets.

Fei Hou received his Ph.D. degree in computer science from Beihang University in 2012. He is currently a research associate professor in the Institute of Software, Chinese Academy of Sciences. He was a postdoc at Beihang University from 2012 to 2014 and a research fellow in Nanyang Technological University from 2014 to 2017. His research interests include geometry processing, image-based modeling, data vectorization, and medical image processing.

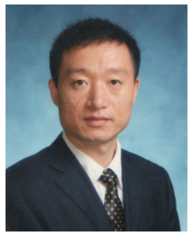

Zhanchuan Cai is a professor in the Faculty of Information Technology, Macau University of Science and Technology, China. His research interests include computer graphics and image processing, multimedia information security, and remote sensing data processing and analysis.

Gang Zhao is a professor in the School of Mechanical Engineering & Automation at Beihang University. He received his Ph.D. degree from Beihang University. His research interests include new geometric modeling methods for curves and surfaces, CAD / CAM, intelligent NC programming technology, and distributed network NC technology.